ICANS IX

INTERNATIONAL COLLABORATION ON ADVANCED NEUTRON SOURCES

22-26 September, 1986

Status Report on the KENS Facility

N. Watanabe, Y. Endoh*, K. Inoue** and M. Misawa

National Laboratory for High Energy Physic,
Oho-machi, Tsukuba-gun, Ibaraki-ken, 305, Japan

* Physics Department, Tohoku University,
Sendai 980 Japan

** Department of Nuclear Engineering,
Hokkaido University, Sapporo 060, Japan

1. Introduction

The pulsed spallation neutron source (KENS) at KEK has successfully been operated with a new uranium target system since last December. Due to improvements in the accelerator and the neutron target, the neutron-beam intensity has been increased by more than four times compared with the previous period in which a tungsten target was used.

Much effort has been devoted to the reinforcement of the biological shielding around spectromertors in order to keep the radiation level in the experimental hall at less than 2 mrem/h.

The beam time allocated to neutron-scattering experiments during the last fiscal year was 750 hours. About forty experiments were carried out successfully among the forty-nine proposals accepted.

This report summarizes the present status of the KENS-I'. The future project is discussed briefly.

2. KENS-I' Program

The KENS-I' Program was aimed at increasing the neutron-beam intensity from the pulsed spallation neutron source KENS-I by one order of magnitude by upgrading the neutron production target from the previous tungsten to depleted uranium, and by improving the performance of the existing proton accelerator (H^- injection as well as increasing the energy of the injector proton linac from 20 MeV to 40 MeV). The final goal for the proton-beam current is hopefully 10 μA at 500 MeV. The macroscopic pulse duration is maintained at about 50 ns at full width. Up to now, a proton beam intensity of about 1.5×10^{12} protons per pulse has already been achieved at a repetition rate 20 Hz as an instantaneous record, corresponding to about 5 μA in time-average current. The accelerators are continuously being tuned to increase the beam current so as to keep the beam loss at an accessible radiation level. At this moment the beam current in routine operation is about two thirds of the maximum value mentioned above in order to make maintenance easy.

The installation of a depleted uranium target system was completed last November; since then it has been operating satisfactorily. Figure 1 shows an illustration of the target assembly which consists of four blocks of depleted uranium enclosed in a bonded clad of zircaloy-2 alloy. The clad uranium blocks were fabricated at Argonne National Laboratory. The uranium core consists of depleted uranium with additions of carbon 450 wt ppm, iron 250 wt ppm and silicon 350 wt ppm. Each target block is a rectangular parallelepiped with partly rounded corners in order to avoid any possible concentration of the thermal stress. The dimension of the block is about 78 mm wide, 57 mm high and 30 mm thick.

The center temperature of the first target block is monitored by a thermocouple. The temperature increase is about 35°C at the rated flow of cooling water 60 ℓ/min for a proton-beam current of 2.5 μA as shown in Fig. 2. This corresponds to a center temperature of 175°C at the rated proton-beam current, well below the design value of 230°C in safety-side estimate by calculations and a mock-up test. At this temperature, thermal stress and thermal-cycling fatigue is no longer important, and we can expect a semi-infinite life of the target.

The gain factor of the neutron production of the depleted uranium target relative to the previous tungsten was measured by thermalized neutrons from the polyethylene moderator at ambient temperature. The

measured gain factor is shown in Fig. 3. The wavelength-dependence of the gain factor may be caused by the difference of the hydrogen density in the moderator, because the previous moderator had a lower hydrogen density (due to radiation damage) than the renewed one. A gain factor 1.9 $\sim$ 2.0 was confirmed from this data.

The cold neutron source, solid methane at about 20 K, has also been renewed. A flat moderator, 12 cm wide, 5 cm thick and 15 cm high, as illustrated in Fig. 4, was again adopted instead of the previous grooved moderator. The reason arises mainly from the limited cooling power of the present refrigerator system. Energy deposition in the previous grooved moderator at the rated beam power (500 MeV x 10 μA) was estimated to be about 50 W, including possible leakage proton bombardment, while the new flat moderator can reduce this value by about 40 %, since the latter has a smaller volume than the former. The new one has a heat exchanger inside the container wall (Fig. 4) instead of an overhead heat exchanger as in the previous system in order to improve the cooling efficiency. A lot of aluminium plates are inserted in the container in order to increase the effective heat conduction in the moderator. A typical moderator temperature in operation is also shown in Fig. 2 where vertical scale shifted by about + 2° K. The ratio of neutron spectrum from the new flat moderator relative to that from the previous grooved moderator is shown in Fig. 5. It is almost flat in the longer wavelength region. The result indicates that the new flat moderator is as good as the previous grooved modelator in the performance of cold neutron production.

One of the most important disadvantage in the use of a uranium target may be increase in the fast-neutron background caused by delayed neutrons. As the worst example, we show in Fig. 6 powder diffraction patterns (one measured with the uranium target and another with the tungsten). These data were obtained using longer-wavelength neutrons (approximately 7 A); the tail part of the spectrum results from the room-temperature moderator. Similar increase of the background was also observed on the WIT (small angle scattering instrument installed directly to the neutron beam hole from the room-temperature moderator). The results indicate that if we utilize longer wavelength neutrons far beyond the Maxwellian peak, the background caused by delayed neutrons becomes predominant. In the case of the inelastic machine the background problem is much more serious. Although the MAX (multi analyzer crystal spectrometer for coherent inelastic scattering) and the LAM-40 (quasielastic machine which is not

incorporated with a neutron guide tube) utilize the main part of the spectrum from the respective moderator, a considerable increase of the background was recognized in the data on these spectrometers. We understand that this is due to an inadequate shield around the incident beam path and insufficient beam collimation for fast neutrons. At KENS we realized a higher coupling efficiency of the target-moderator by adopting a target shape of a rectangular parallelepiped with a possible minimum distance between them. This configuration, however, is more susceptible to the background caused by delayed fast neutrons. A great deal of effort must be put to overcome this problem.

3. Improvements of Spectrometers

During the past two years a great effort was expended in developing a new type one-dimensional ^{6}Li-loaded-glass scintillation position-sensitive detector,[1] PSD, using a light-encode method. The detector system was completed last summer and installed at the four-circle single-crystal diffractometer (FOX). After electrical tuning, the detectors were successfully operated.

The layout of the PSD is shown Fig. 7. One detector element consists of 3 cylindrical scintillators (3 mm in diameter and 30 mm in hight). Flexible plastic optical fibres (3 mm in diameter) are connected to both ends of the scintillator. A total of 384 scintillator elements sit side by side in a semicircle 45 cm in radius. The PSD is divided into two sections, that is, right and left sections. Each section has 64 detector elements (192 scintillators), and they are covered by 12 PMs. Data in each section are further divided into 4 blocks. The positional resolution of the PSD was determined to be 9.7 mm. The resolution does not depend on the position since the shape of the PSD is semicircular and the scattered neutrons from the specimen never strike the detector elements obliquely.

One example of the raw data is shown in Fig. 8. The specimen is a well known material, $BaPb_{0.7}Bi_{0.3}O_3$, the size of which is 1 mm x 1 mm x 2 mm. The peak intensity of 200 reflections is 35,000 cts/10 μs for 4 hours. The analysis gave us a satisfactory parameters regarding structure refinement.

The construction of the thermal neutron small angle scattering instrument (WIT)[2] has partly been completed with a pilot detector system. The instrument has been installed at the H-2 neutron beam hole which

directly views the polyethylene moderator at room temperature. The schematic drawing is given in Fig. 9. The instrument is equipped with a two dimensional converging Soller slit and 12 annular ^{6}Li glass scintillation detectors. The FWHM of neutron beam size at the focusing point is observed as 9 mm x 9 mm without escape ghosts. The 12 annular detectors are located at the scattering angles between 0.46° and 4.88° and can cover the Q range from 0.008 A^{-1} to 1.34 A^{-1} by use of the wavelength between 0.4 Å and 6 Å. The construction will be completed by this year.

Change of the cold moderator from the grooved to the flat brought great advantage to the performance of the high-resolution powder diffractometer (HRP). The resolution $\Delta d/d$ was improved from 0.40 to 0.30 %. The simpler form of the peak shape function from the flat moderator made it possible to establish a Rietveld program[3] for analyzing powder patterns from the HRP. The HRP simultaneously utilizes a wide range of neutron spectrum 0.5-10 A. Correspondingly, the pulse shape function of neutrons significantly varies with neutron wave length : from a narrow and more symmetric one at the 1/E region to a broad asymmetric one at the Maxwellian region of cold neutrons, passing through a more complex shape at the transient region. It is very important to use a neutron shape function expressed by a unified set of parameters over the entire range of wavelength. We used a peak shape function of Cole and Windsor type,[4] but modified it based on a new pulse shape function by Ikeda and Carpenter.[5] The peak shape is described in terms of three separate regions: leading side with a Gaussian function, trailing side with another Gaussian function and trailing edge expressed by mixing two exponential functions. The mixing ratio changes with neutron wavelength; the steeply decaying exponential function is dominant in the short wavelength region, while the slowly decaying function becomes major with increasing wavelength. Figure 10 shows a diffraction pattern from Al_2O_3 together with calculated Rietveld profile. The pattern covers a d-range of 50 - 350 pm and includes 274 reflections. Final R-factors are R_{wp} = 7.1 %, R_p = 4.9 %, R_B = 1.9 % and R_F = 1.8 %.

The polarized epithermal neutron spectrometer (PEN) is one of the most challenging machine in our facility. The polarized epithermal neutrons with the polarization of 70 % or more are normally produced by a dynamically polarized proton filter.[6] As a unique use of the polarized

epithermal neutrons, measurements of parity non-conserving effect in nucleus were carried out. This is well demonstrated in Fig. 11 where helicity dependence of the resonance of the neutron radiative capture reaction of ^{139}La observed with the PEN[7] is shown. The preliminary result of asymmetry in the γ-ray intensity was obtained to be (9.5 ± 1.2) %.

The three LAM-Type quasielastic / inelastic scattering spectrometers (LAM -80, LAM-40 and LAM-D) are the busiest ones in our facility. About 1/3 of the proposals approved this year are allocated to these machines. One of the three machines, inelastic scattering spectrometer LAM-D, has only one analyzer mirror, but is scheduled to be upgraded. The new machine will have four analyzer mirrors as shown in Fig. 12. The machine can cover the range of energy transfer below 100 meV with a constant energy resolution of which typical value is about 0.3 meV for elastic scattering (4.3 meV).

Some of the interesting measurements recently done by use of these machines are (1) quasi-elastic scattering of a super cooled water measured with LAM-40, (2) quasi-elastic scatterings of polyethylene and polybtadiene measured with LAM-80 above their melting points, of which Q dependence were quite different with each other and (3) low energy excitations measured with LAM-40, which are commonly observed in various kinds of disordered states including organic amorphous polymers and inorganic glasses.

A series of chopper phasing experiments to the accelerator (500 MeV synchrotron) were carried out extensively with a newly developed phasing circuit. Since the frequency of the synchrotron is not exactly constant, it is an inevitable task to keep the chopper, with its high moment of inertia, sufficiently in phase with the synchrotron to achieve a better time-of-flight resolution. Within the acceptable time band (≃ 50 μs centered at peak field in the synchrotron magnet), the proton beam can be extracted according to the request from the chopper. If the request is outside the band, the beam is automatically extracted at the end of the band. Though the phase fluctuation of the chopper is about ± 20 μs at 400 Hz, we have achieved a phased extraction within a time accuracy of ± 0.4 μs with a duty cycle of more than 99 %. The performance is sufficiently good for a practical use. The design work on the chopper spectrometer

(INC) is now in progress.

The other instruments (HIT, SAN, MAX, RAT, TOP) run well as usual without great improvement of the instruments this year.

4. Future Program KENS-II

As a next generation neutron source in Japan we proposed an intense pulsed spallation neutron source so called KENS-II. The proposal included the construction of a high intensity proton synchrotron which was also supported by the μSR group. The whole project including a future program of the μSR as well as the name of the accelerator are then called GEMINI (a Generator of Meson Intense and Neutron Intense beam). For past five years the design studies of the accelerator system have extensively been performed.[8,9] The design goal of the synchrotron was 800 MeV with a time average beam current 500 μA and with a repetition 50 Hz. Recently scientists in the field of nuclear physics have proposed a future program so called Super Hadron Project aiming to produce intense kaon and anti-proton beam. Since then the both projects are being unified. Now KENS-II project is getting a wide range support among the Japanese scientists and expected to be authorized as a part of the Super Hadron Project.

The accelerator system in this program is still open, but may consist of a proton linac, a first ring accelerator for neutron and pion production which corresponds to the previous GEMINI part, with a storage ring for nuclear physics, and a 20 - 30 GeV ring accelerator for kaon and anti-proton factory. In the first phase of the project the existing 12 GeV proton synchrotron will substitute the 20 - 30 GeV ring accelerator after a necessary upgrading. Requirements for the first ring accelerator are of wide variety group by group. Neutron group requests pulsed proton beam with lower energies (<1.5 GeV) and a repetion rate not larger than 50 Hz but with possible highest beam current, while μSR people do with higher energies (>1.5 GeV), better emittance and with more frexibility in pulse width and repetition rate. The nuclear physics group requests higher energies 3 GeV or more and some times stretched beam, of course, with better emittance.

In order to make our standpoint more clear we performed a neutronic computor simulation for various proton energies in the range 0.5 - 3 GeV,

using a high energy transport code NMTC/JAERI.[10] As a model target, we assumed a cylindrical target, 10 cm in diam. and 32 cm (64 cm for 3 GeV) long, which consists of many disks of depleted uranium enclosed in a bonded clad of zirconium with proper cooling water gaps. Beam profile of protons incident upon the target was assumed to be cylindrical, 4.7 cm in diam. which may be typical for high intensity proton beam.

Figure 13 shows the total neutron yield for various proton energies. Neutron yield is almost proportional to the incident proton energy below 1 Gev, but there is no advantage for energies much greater than about 1 GeV. 3 GeV proton produces only two times as many neutrons as 0.8 GeV proton. Figure 14 shows axial distributions of source neutrons integrated over the radial direction. The maximum luminosity is almost unchanged with increasing proton energy. For reference, Fig. 15 shows spatial distributions of energy deposition in the target. Maximum heat load is also unchanged with proton energy.

Thermal neutron beam intensity was calculated using the TWOTRAN-II. In the two dimensional calculation, we assumed an annular water moderator, 10 cm wide and 5 cm thick, surrounding the target with a beryllium reflector 30 cm thick in the remaining part of the target cylinder, instead of a reference moderator 10 x 10 cm^2 x 5 cm thick as usual. Table I summarizes a rough estimate on relative intensity of thermal neutrons from the moderator for various proton energies.

We decided from the result that the acceptable maximum proton energy for pulsed neutron research, as a consequence of compromise with other group, is around 1.5 GeV.

The energy of the injector proton linac is another crucial point in the discussion. The nuclear physics group is keen to have a higher energy, hopefully 1 GeV, in order to obtain proton beam with better emittance from a synchrotron. The maximum energy of the injector, of course, depends on the total budget available. An injection energy of 100 MeV was considered in the original GEMINI, but higher injection energy is welcomed also in the first ring. Fox example 300 MeV injection will largely improve the performance of the first ring accelerator.

References

1) N. Niimura, J. de phys. (1986) in press ;
N. Niimura, K. Yamada, T. Kubota, M. Isobe, F. Okamura, I. Kawada, A. Masaki and H. Horiuchi, J. appl. Cryst. to be published.

2) N. Niimura, A. Ishida, M. Ueno, K. Yamada, M. Hirai and K. Aizawa, KENS-VI (1986) to be published.

3) F. Izumi: KENS Report-VI (1986) to be publoshed.

4) I. Cole and C. G. Windsor: Nucl. Instrum. Method, 171 (1980) 107.

5) S. Ikeda and J. M. Carpenter: Nucl. Instrum. Methods, A239 (1985) 536.

6) Y. Masuda, S. Ishimoto, M. Ishida, Y. Ishikawa, M. Kohgi and A. Masaike, submitted to Nucl. Instrum. Meth.

7) Y. Masuda, T. Adachi, S. Ishimoto, E. Kikutani, H. Koiso, K. Morimoto and A. Masaike: Hyperfine Insteractions to be published.

8) H. Sasaki and GEMINI study group : proc. ICANS-VII, AECL-8488 (1983) 50.

9) Y. Ishikawa and the KENS group : proc. ICANS-VIII, RAL-85-110 (1985) 17.

10) Y. Nakahara : J. Nucl. Sci. Technol., 20 (1983) 511.

Table I Thermal Neutron Yield

Ep (GeV)	Thermal Neut. yield (arb. unit)	Total No. of Source Neut.
0.8	59.8	3962
1.5	82.85	6010
2.0	96.97	7119
3.0	106.03	8199

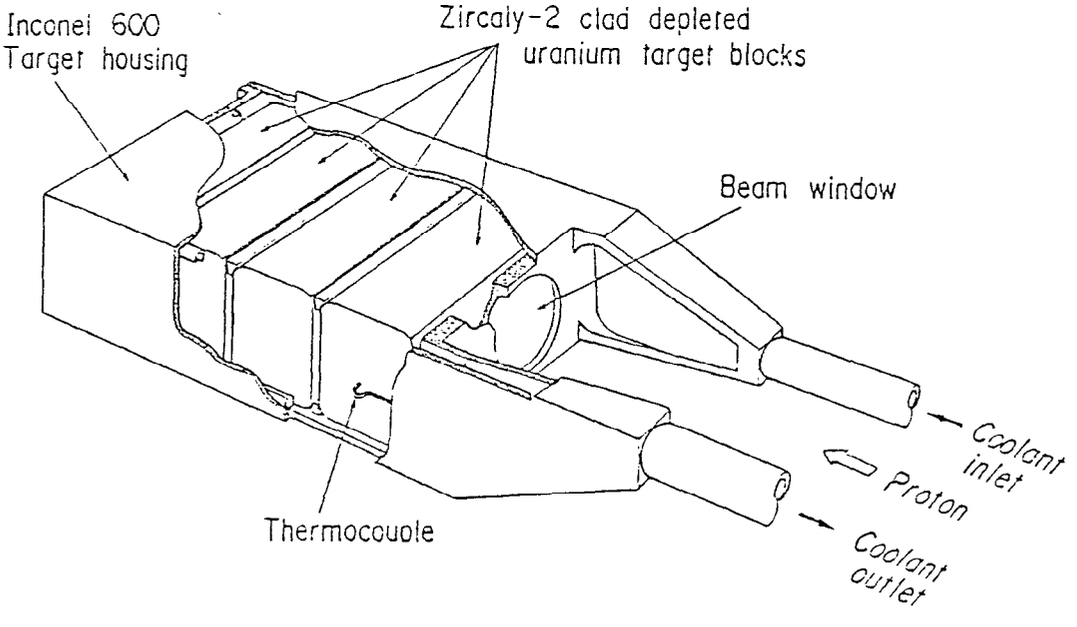

Fig. 1 Illustration of the target assembly which consists of four blocks of depleted uranium enclosed in a bonded clad of zircaloy-2 alloy. Target hausing is made of Inconel 600.

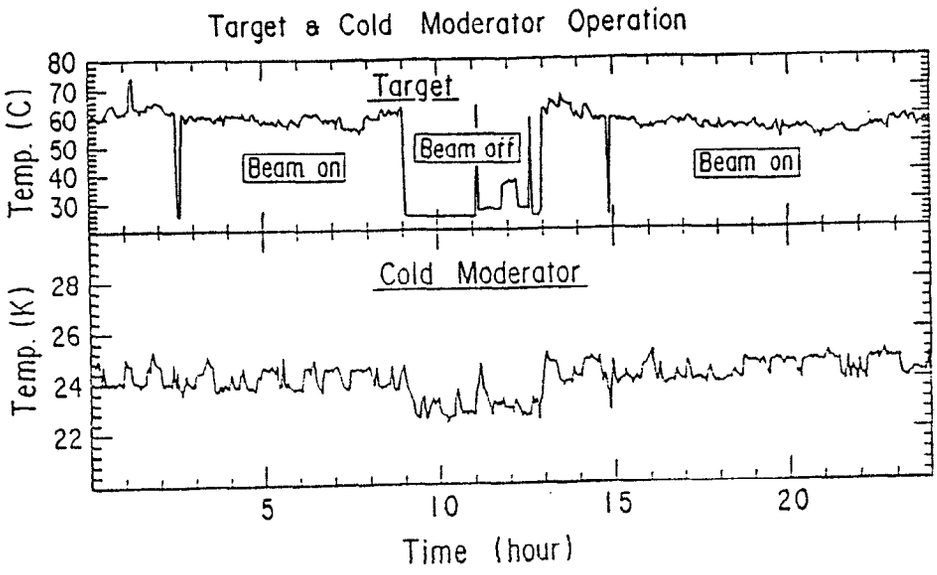

Fig. 2 Operational characteristics of the target and the cold moderator at a proton-beam current of 2.5 μA : center temperature of the first target block (upper figure), temperature of the solid-methane moderator (lower figure).

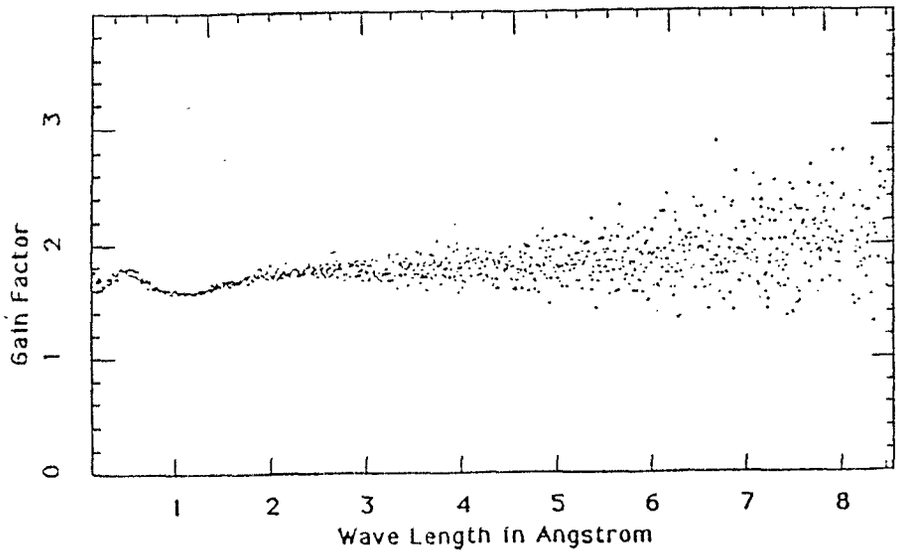

Fig. 3 Neutron gain factor of the uranium target relative to the previous tungsten determined by thermalized neutrons from the polyethylene moderator at ambient temperature.

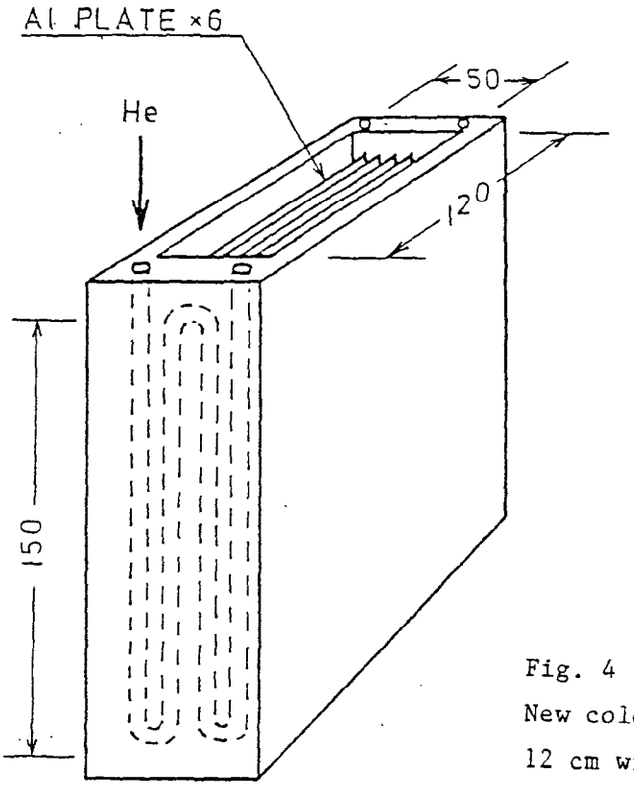

Fig. 4
New cold moderator container, 12 cm wide, 5 cm thick and 15 cm high.

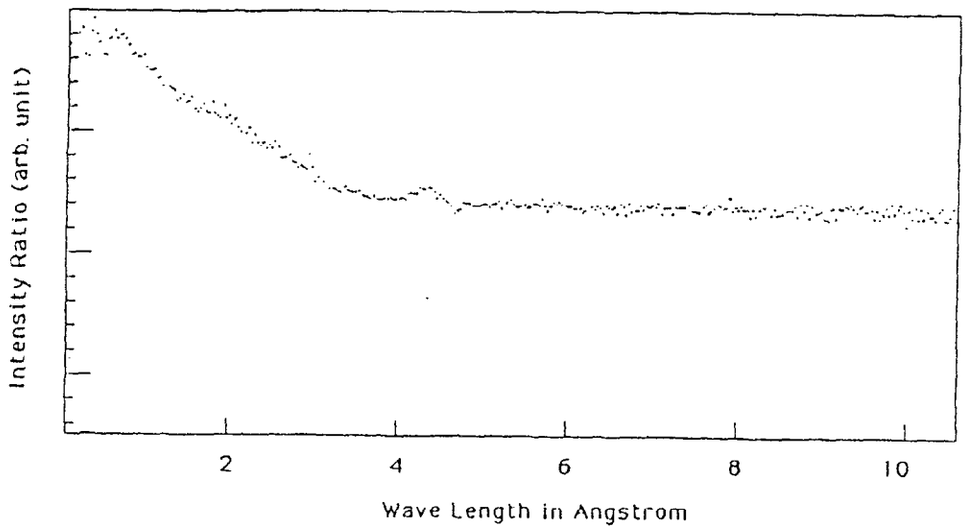

Fig. 5 Ratio of the cold-neutron spectrum from the new solid-methane moderator to that from the previous grooved one.

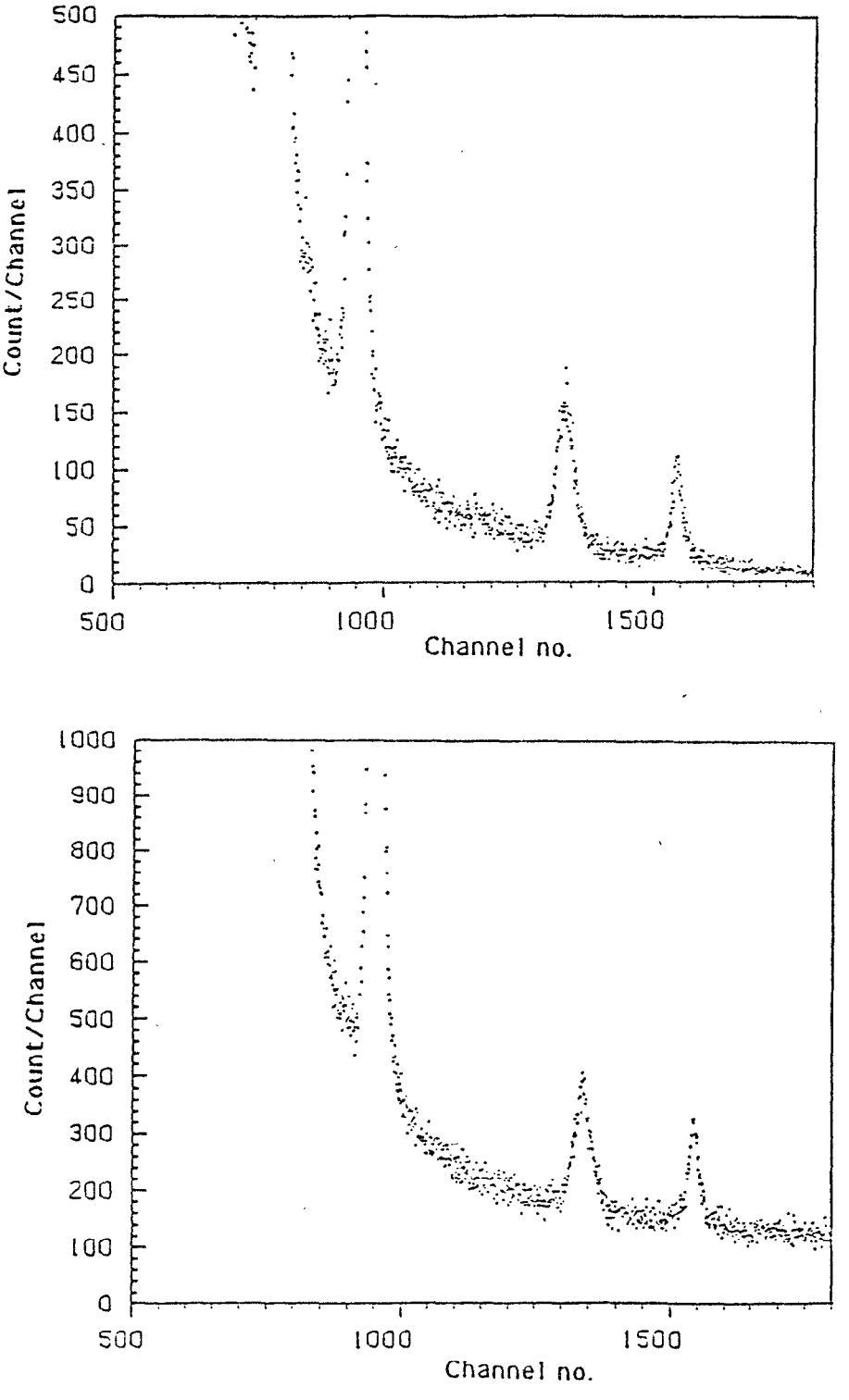

Fig. 6 Comparison of the background level in powder diffraction (worst example) : with a tungsten target (upper figure), with a uranium target (lower figure). The higher background in the uranium is due to delayed neutrons.

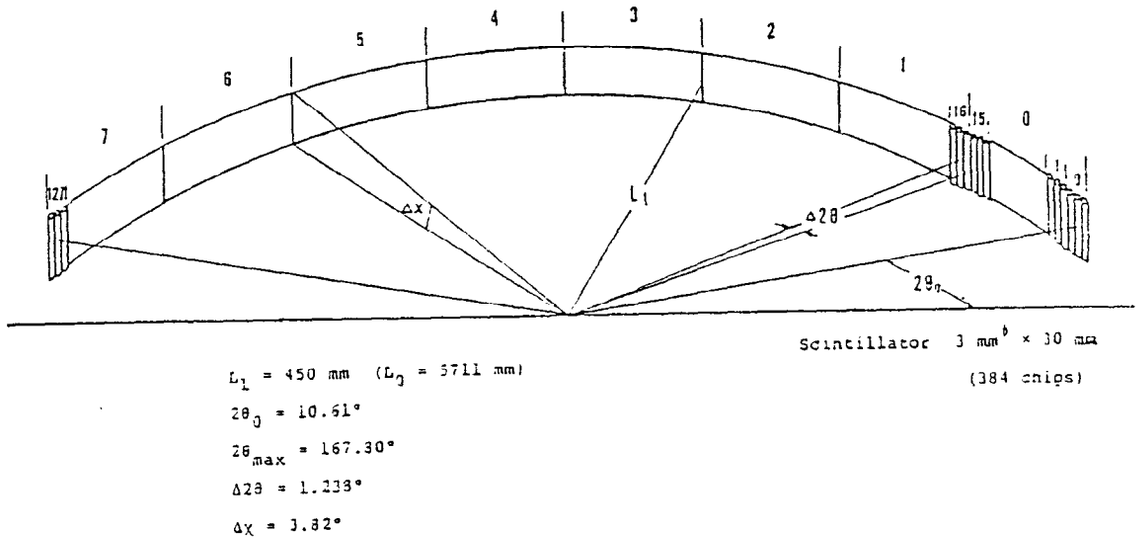

Fig. 7 Layout of a one-dimensional PSD using a ^{6}Li-glass scintillator installed at the single-crystal diffractometer FOX.

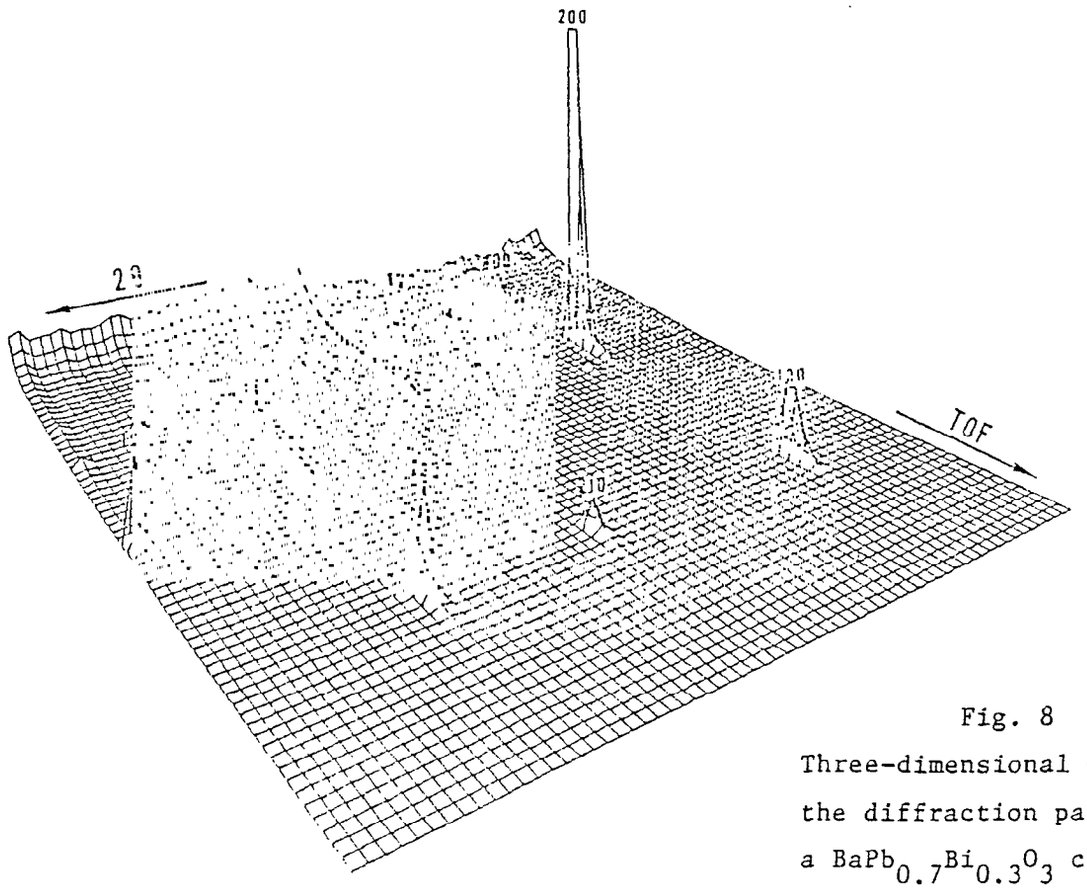

Fig. 8
Three-dimensional display of the diffraction pattern from a $BaPb_{0.7}Bi_{0.3}O_3$ crystal (1 mm x 1 mm x 2 mm).

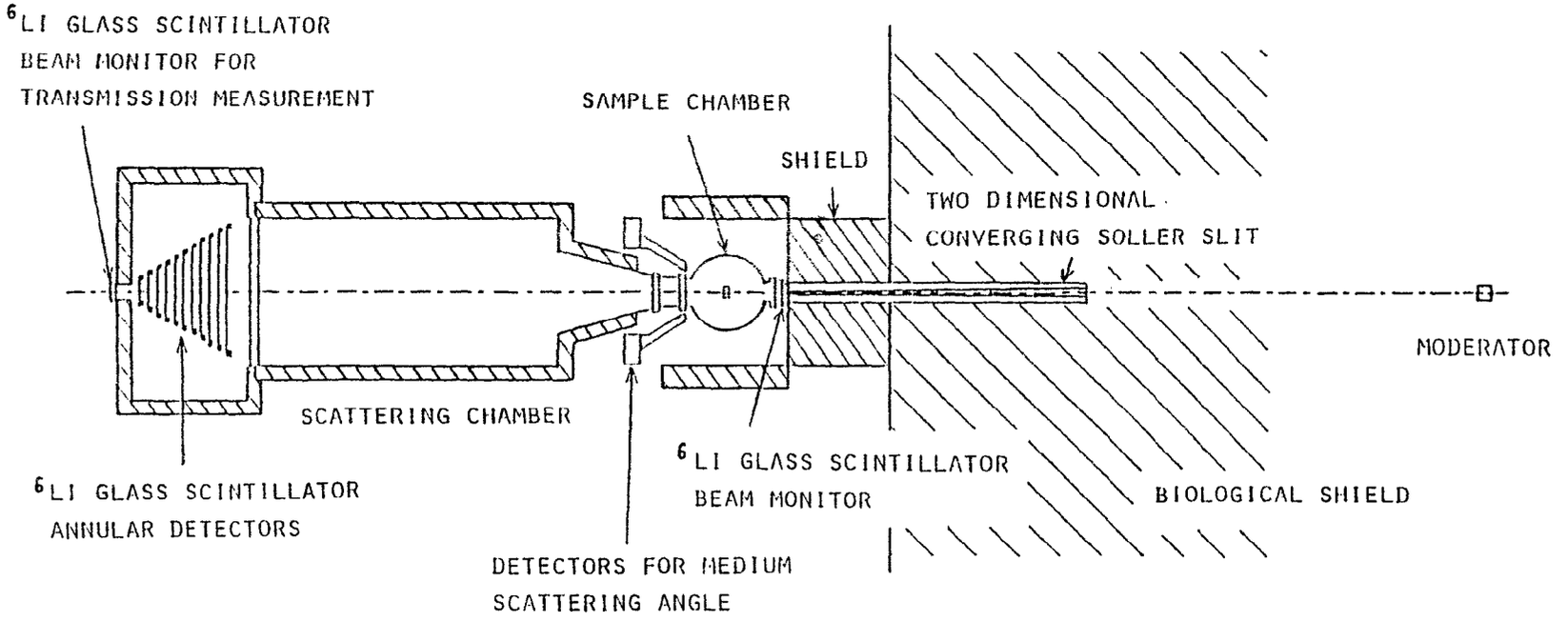

Fig. 9 Schematic layout of WIT.

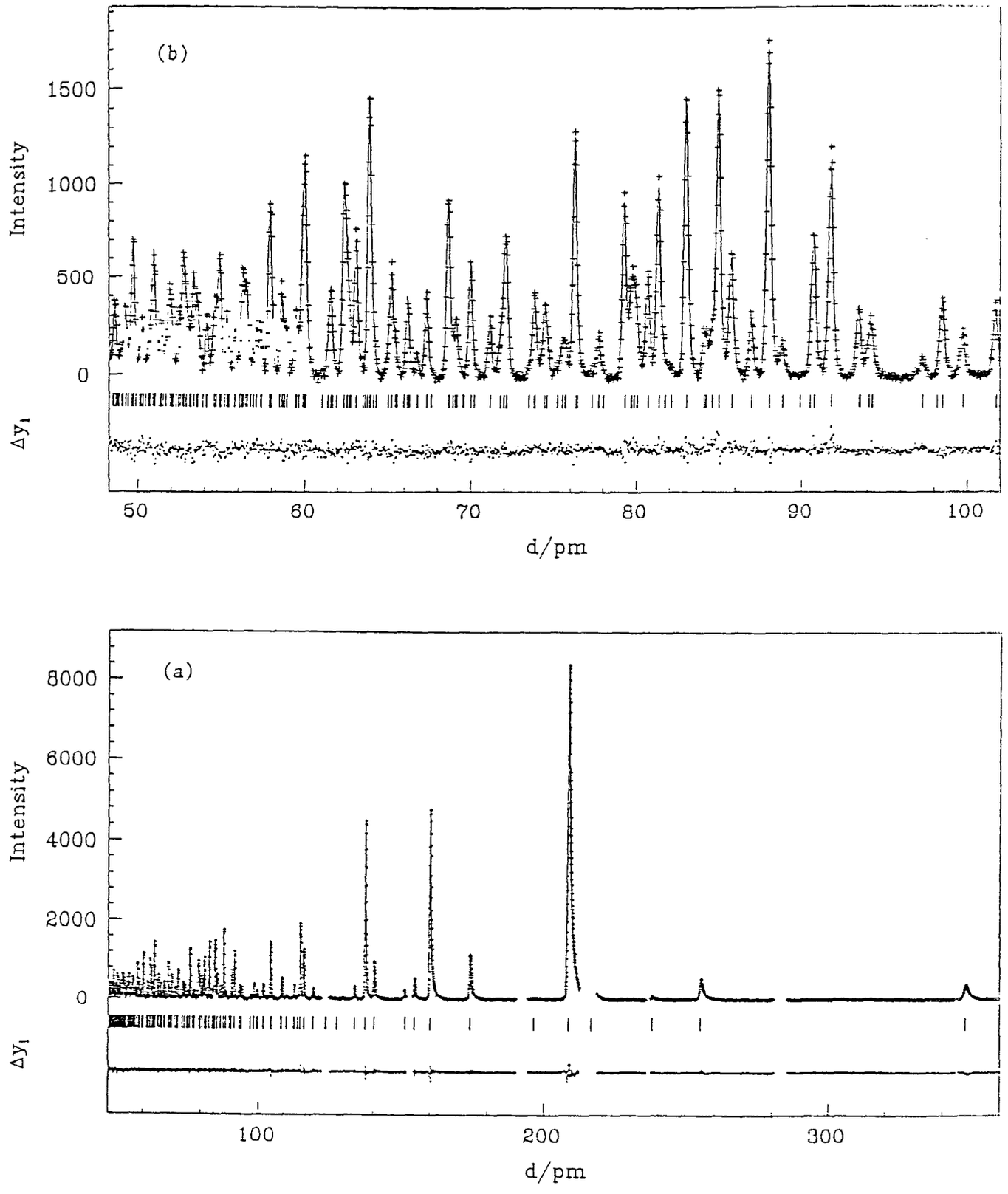

Fig. 10 (a) Neutron diffraction patter of Al_2O_3 observed with the HRP. Regions where Bragg reflections of the vanadium sample holder appear are omitted.
(b) Enlarged portion in the range d = 50 - 100 pm. Background is subtracted.

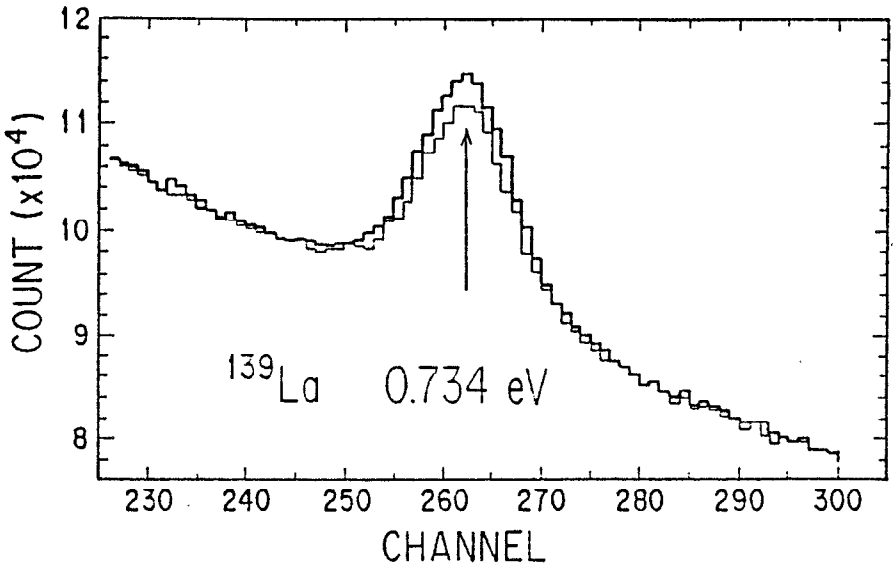

Fig. 11 TOF spectra around 0.743 eV resonance of ^{139}La observed with the PEN. The thick and thin lines are refer to the spectra for the parallel and antiparallel neutron polarization to the beam, respectively.

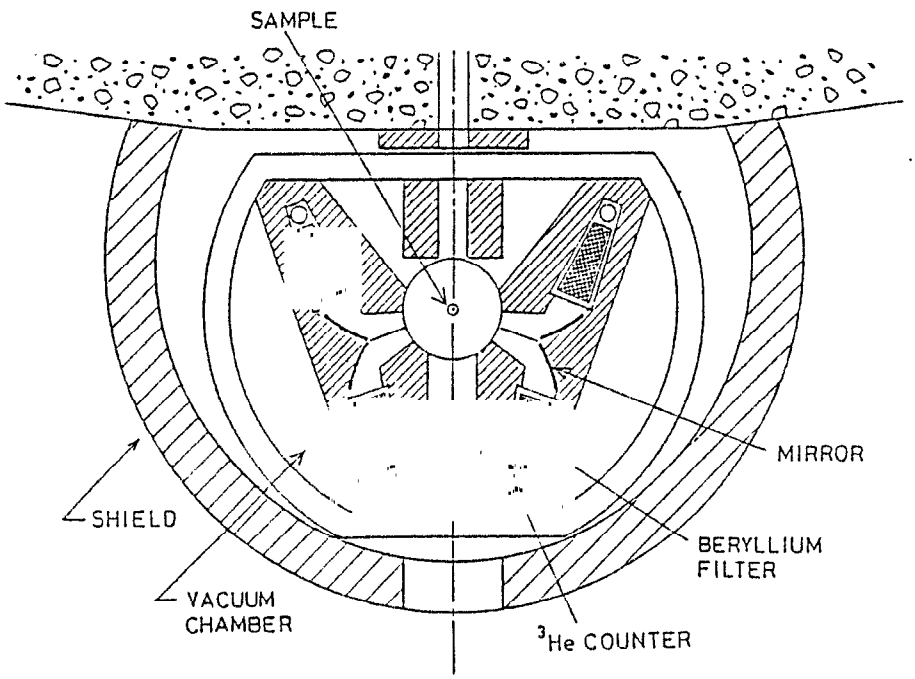

Fig. 12 Schematic layout of a new LAM-D.

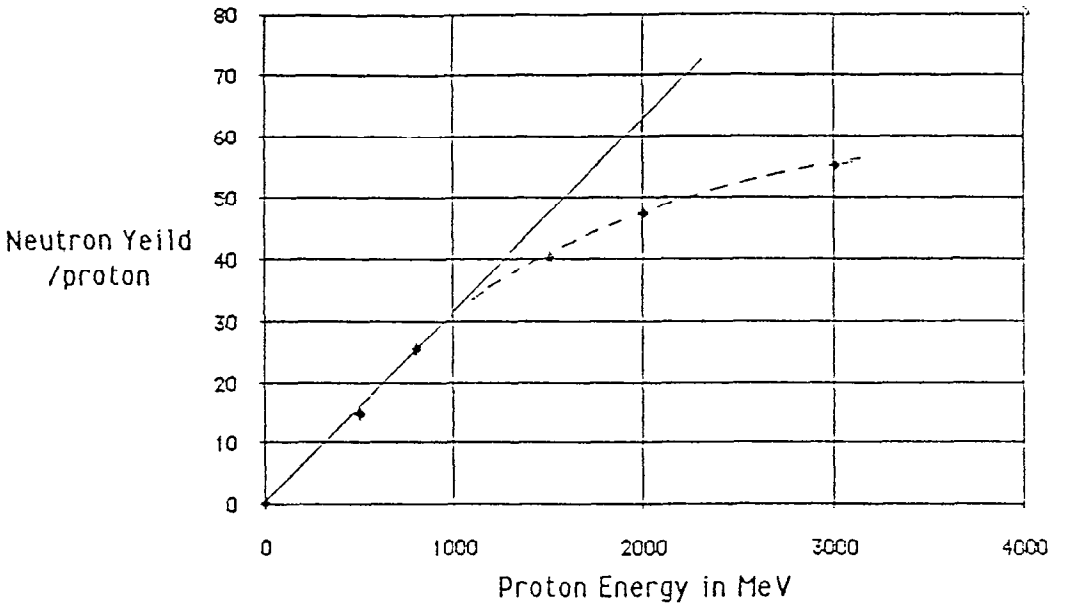

Fig. 13 Neutron total yield vs proton energy.

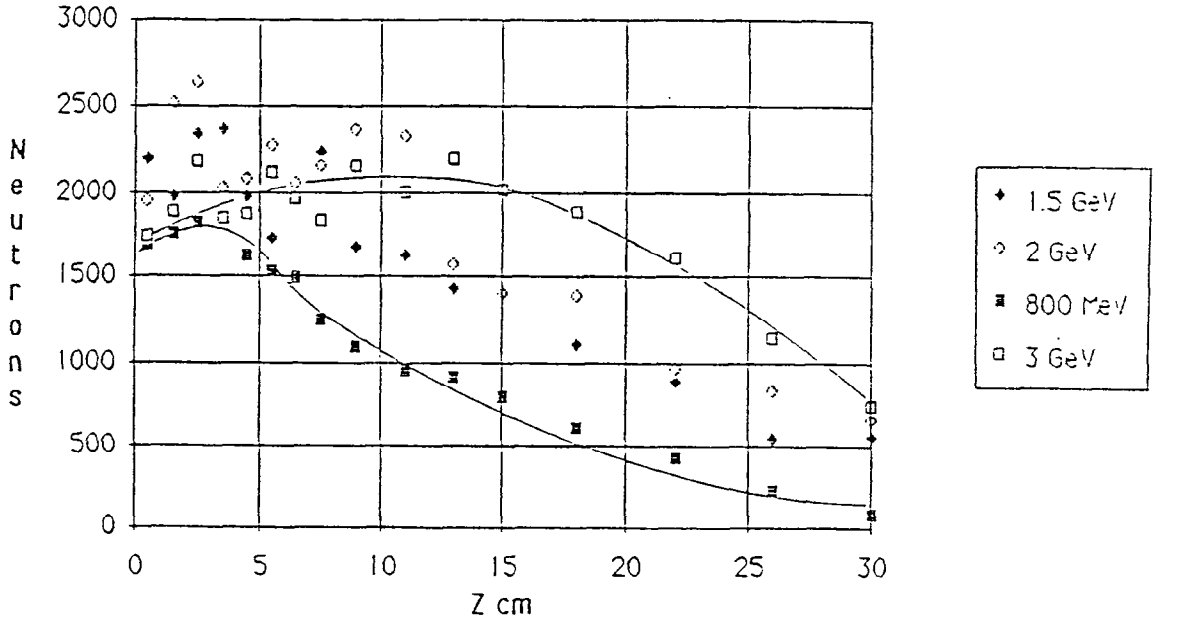

Fig. 14 Axial distribution of source neutrons for various proton energies.

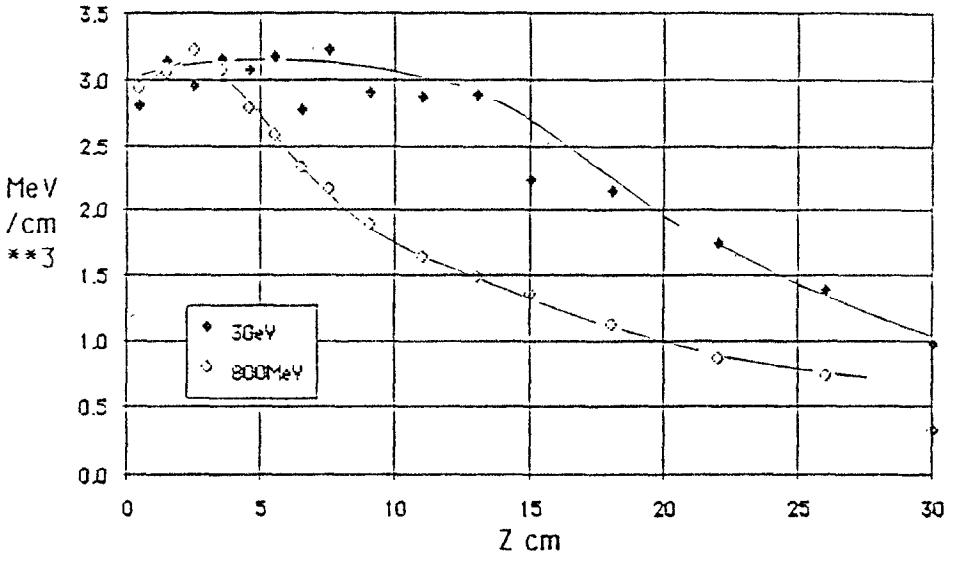

Fig. 15 Spatial distribution of energy deposition for different proton energies.